



HAL
open science

Synoptic assessment of water resource variability in reservoirs by remote sensing: General approach and application to the runoff harvesting systems of south India

François Mialhe, Yanni Gunnell, Catherine Mering

► To cite this version:

François Mialhe, Yanni Gunnell, Catherine Mering. Synoptic assessment of water resource variability in reservoirs by remote sensing: General approach and application to the runoff harvesting systems of south India. *Water Resources Research*, 2008, 44 (5), 10.1029/2007WR006065 . hal-04604349

HAL Id: hal-04604349

<https://hal.science/hal-04604349>

Submitted on 7 Jun 2024

HAL is a multi-disciplinary open access archive for the deposit and dissemination of scientific research documents, whether they are published or not. The documents may come from teaching and research institutions in France or abroad, or from public or private research centers.

L'archive ouverte pluridisciplinaire **HAL**, est destinée au dépôt et à la diffusion de documents scientifiques de niveau recherche, publiés ou non, émanant des établissements d'enseignement et de recherche français ou étrangers, des laboratoires publics ou privés.

Synoptic assessment of water resource variability in reservoirs by remote sensing: General approach and application to the runoff harvesting systems of south India

François Mialhe,¹ Yanni Gunnell,² and Catherine Mering¹

Received 27 March 2007; revised 24 September 2007; accepted 13 February 2008; published 16 May 2008.

[1] This paper presents a methodological procedure based on remote sensing and image analysis techniques designed to map and quantify water stocks in small irrigation reservoirs over vast, user-defined regions. Because the method is based on unsupervised pixel classification schemes, it is analytically transparent and entirely replicable and can therefore be used in most settings as a tool for integrated water resource management, planning, or policy making, with benefits to irrigation, land use, agriculture, and water-related social issues. Satellite images of semiarid south India are used here to quantify fluctuating water volumes in ~2500 reservoirs. In this pilot study, the detection of temporal trends and spatial discontinuities in land use at successive dates within reservoir beds is a proxy for assessing the performance of reservoirs and for formulating hypotheses on the environmental, socioeconomic, or anthropological reasons behind the inferred levels of infrastructural maintenance or disuse. The synoptic approach paves the way for future efforts as better ground truth data become available.

Citation: Mialhe, F., Y. Gunnell, and C. Mering (2008), Synoptic assessment of water resource variability in reservoirs by remote sensing: General approach and application to the runoff harvesting systems of south India, *Water Resour. Res.*, 44, W05411, doi:10.1029/2007WR006065.

1. Introduction

[2] Resolutions formulated at the 2003 Kyoto World Water Forum establish that water resource management should shift its long-standing emphasis on regulation by government to regulation by governance. Advocacy for notions such as integrated water management and participatory irrigation is now widespread. This recent approach encourages a revival of the common-property approach to water resources [e.g., Sakurai and Palanisami, 2001], which has been prevalent for centuries in some rural communities around the world [e.g., Barrow, 1999; Gunnell and Anupama, 2003], and promotes water user associations. With this focus in mind, natural resource inventories and land capability surveys for fine-scale watershed management require that a consensus be reached on a limited range of methods and standardized land classification categories in order to facilitate research, information transfer, training, and planning.

[3] An increase in the productivity of water in response to growing populations and water demand in dry areas of the semiarid tropics in particular requires a search for techniques designed to monitor water availability and system efficiency and to map problem areas for policy intervention and adaptive management. South India is one region of the world where water-harvesting reservoirs are widespread and

is the chosen setting in which the methodology developed here has been implemented. This paper uses this region (Figure 1) as an example to show how the synoptic qualities of satellite imagery help to obtain quantitative estimates of water stocks in reservoirs.

[4] In south India, tanks are traditional water storage reservoirs designed to harvest and store rainfall and surface runoff (Figure 2). They are designed to mitigate the impact of seasonal and interannual rainfall variability on water by extending its availability for agriculture through storage. So-called nonsystem tanks are supplied by small catchments that capture overland flow and that may include irrigated land. They lack access to perennial water sources unless they are supplied by a perennial river via a canal, in which case they are known as system tanks. Strong evaporative losses during the dry season and no carryover of live storage between seasons also mean that stocks are entirely depleted and varyingly replenished on a yearly basis.

[5] Tank irrigation is profitable, particularly to small farmers [Palanisami and Meinzen-Dick, 2001; Balasubramanian and Selvaraj, 2003], and its sustainability in India is reflected in its 2000-year history [Gunnell et al., 2007]. These reservoirs are widespread in the states of Andhra Pradesh [Prasad et al., 1993; Rao et al., 1993; Rao and Chakraborti, 2000], Tamil Nadu, and Karnataka [Palanisami and Meinzen-Dick, 2001]. In Tamil Nadu, ~39,000 tanks command ~30% of the total irrigated land area [Anbumozhi et al., 2001; Ranganathan and Palanisami, 2004], but this ratio has been declining in the last 25 years because of a range of socioeconomic causes broadly related to demographic pressure, the decline of surface water as a common property resource, extended periods of drought [Gunnell et al.,

¹Department of Geography, UMR 8586, CNRS, Université Paris VII-Diderot, Paris, France.

²Department of Geography, UMR 8591, CNRS, Université Paris VII-Diderot, Paris, France.

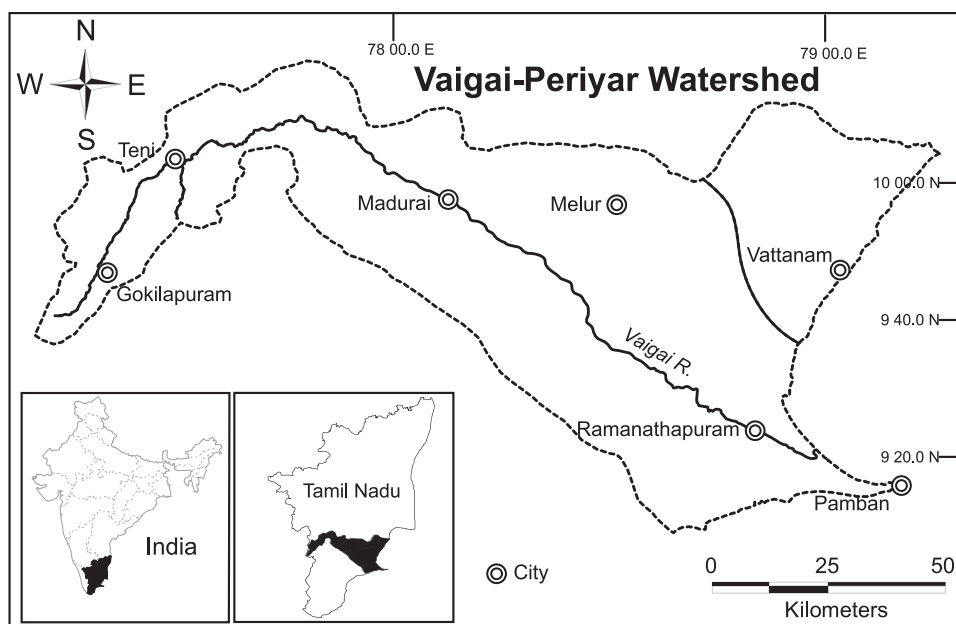


Figure 1. Study area.

2007], and, more generally, poor governance [Mosse, 1997; Palanisami and Meinzen-Dick, 2001; Sakurai and Palanisami, 2001; Balasubramanian and Selvaraj, 2003; Sharma, 2003; Kajisa et al., 2004].

[6] Extensive water-harvested areas can be readily monitored from space at minimal cost. In spite of the existing technology to do so, however, synoptic, spatially distributed quantitative analyses of surface water resources based on remote sensing are uncommon [Ambast et al., 2002]. Existing work on reservoir mapping tends to rely on supervised classifications [e.g., Liebe et al., 2005], which require a training data set and are therefore costly and time consuming in field work prior to image processing. Water harvesting in India has been studied mostly from the ground by social scientists, economists, and agronomists. Field-based case studies are predominantly concerned with land tenure, social anthropology, or cost-benefit and viability analyses on a local scale [Palanisami and Easter, 1987; Vaidyanathan, 2001; Mosse, 2003]. Rare literature on the hydrology of reservoir irrigation mostly deals with water mass balance at the single-reservoir scale [e.g., Jayatilaka et al., 2003; Li and Gowing, 2005] using a range of local-scale environmental data that are often unavailable in many regions of the world. What such models gain in quantitative precision they therefore lose in breadth, swiftness of implementation, and applicability as decision- and policy-making

tools. Here we develop an analytically transparent and replicable methodology based on unsupervised classification schemes with potential for use in other settings around the world.

2. Method

2.1. General Approach

[7] Tank storage is extremely sensitive to rainfall variability and is vulnerable to abstraction losses. Water in tanks is retained after the end of the rainy season, which extends from late September to early January (Figure 3a) for a period ranging from weeks to months that also depends on soil properties and water consumption rate. When analyzed using satellite images with comparable anniversary registration dates, the state of an individual tank at the end of the rainy season can provide an appreciation of its economic performance.

[8] Over time, tank storage capacity diminishes because of siltation, but this and other negative impacts can be redressed by periodic desilting work, which has kept the system in operation for centuries. Therefore, once climatic variability has been filtered out as a contributing factor to observed reservoir water levels, land cover changes within tank beds and trends in water levels represent two good proxies for appraising levels of collective involvement in

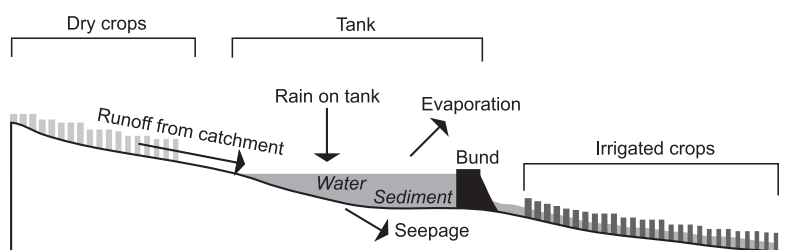


Figure 2. Schematic cross section of a tank. Topographic slope is greatly exaggerated.

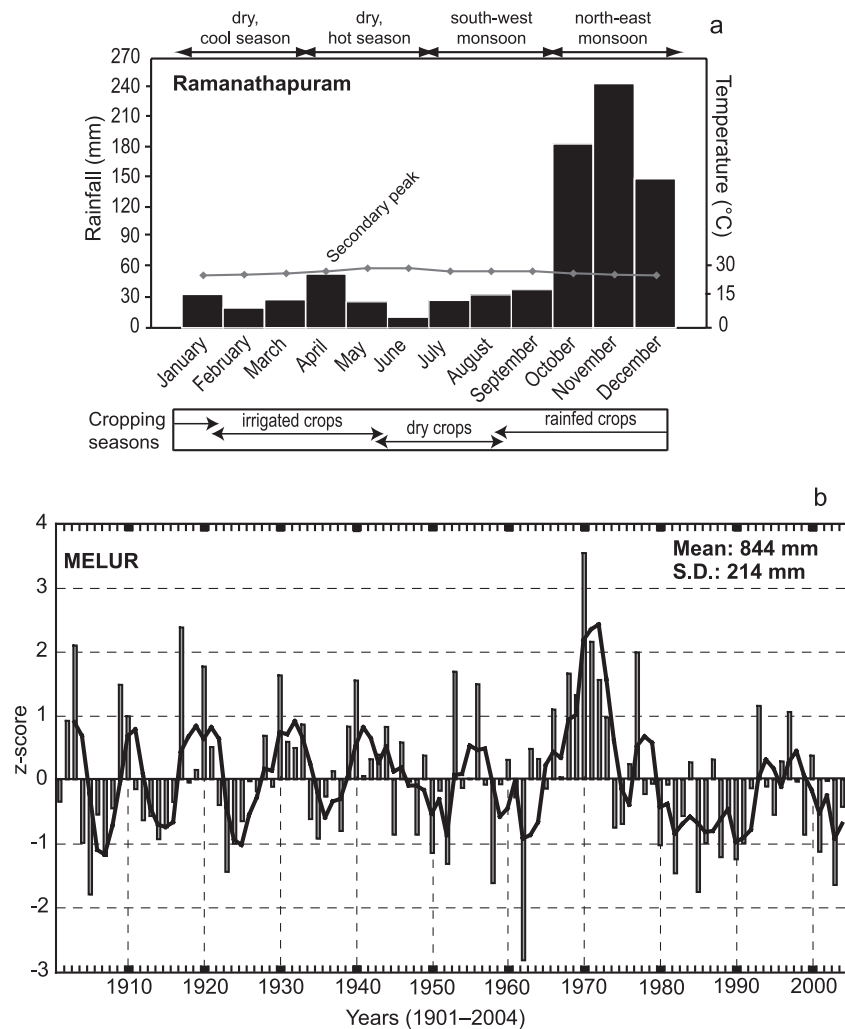


Figure 3. Climate in study area. (a) Rainfall diagram of Ramanathapuram (located in Figure 1), representing the seasonal cycle throughout the study area. (b) Normalized interannual variability of rainfall at Melur (see Figure 1), here based on a 103-year instrumental rainfall record. Black curve is 3-year moving average.

maintaining reservoir efficiency at individual reservoir to regional scales. An estimate of reservoir storage can be calculated in geographic information system (GIS) based maps of aquatic surface areas obtained by terrain classification algorithms, with scope for producing a database of water stock fluctuations indexed on rainfall surpluses or deficits from year to year over broad regions. Independent knowledge of mean reservoir depths can be used to calculate volumetric water stocks. Error on estimates is inevitable but can be mitigated when possible by field data.

[9] This kind of data is particularly useful to water planning and agricultural forecasting bodies in settings like India, where statistics on tanks are either unavailable or poorly integrated because responsibility for tank management is split between several independent administrations. Contingency plans for famine relief and the need for compensatory efforts in other forms of irrigation (river-fed reservoirs and groundwater irrigation) can be better anticipated. Another benefit accruing from synoptic knowledge of surface water reserves is that it can also assist politicians in exhorting farmers to modulate the exploitation of ground-

water reserves, which in India are increasingly being mined to critically unsustainable levels as an open access resource insufficiently regulated by legislation.

2.2. Image Selection and Use of the Rainfall Record

[10] The Vaigai basin (Figure 1) drains an area of 7393 km² with a mean population density of 300 inhabitants per square kilometer. Over 50% of the working population is employed in agriculture; that is, ~1 million people are directly dependent on water for agriculture. The coastal plain to the north, which does not belong to the Vaigai watershed, was also included in this study because it is one of the historical heartlands of tank irrigation in south India and displays such a high spatial density of tanks that little room is left for other forms of land use or natural habitat (Figure 4).

[11] Rice is both the staple food and the principal agricultural product in the study area. In Tamil Nadu, rain-fed paddy crops (samba season) are sown in September and harvested in January. During the navarai season (January to April), a second, reservoir-irrigated crop may be

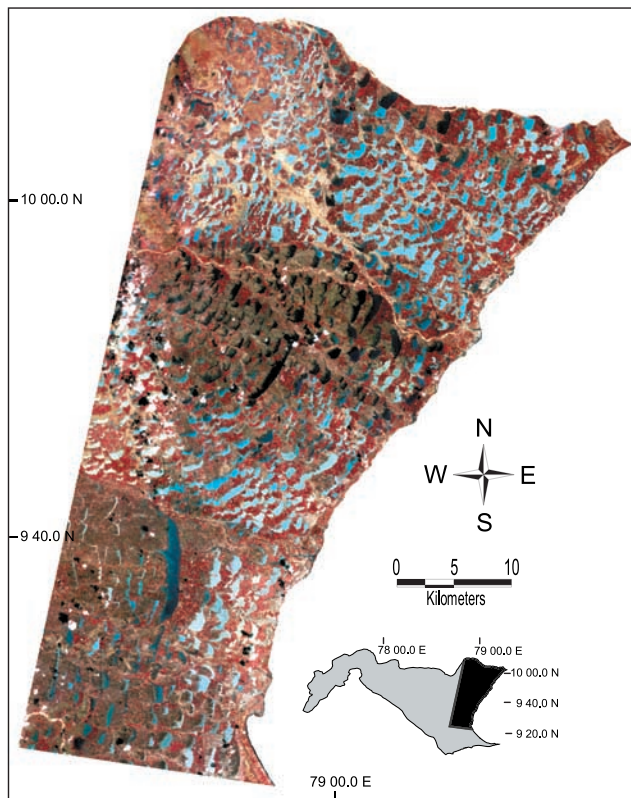


Figure 4. False color composite (red-green-blue: NIR-red-green) of the northeast part of the study area using the 21 January 1979 MSS image. Note differences in tank shape where thin, crescent-shaped water bodies tend to indicate loss of tank capacity due to siltation. In such cases, residual accommodation space for water occurs immediately behind the tank bund.

attempted if reservoir storage has been adequately replenished by rainfall during the preceding wet season.

[12] Independent knowledge of rainfall data is critical because it allows comparison of reservoir levels of the same area during different years and helps to discriminate between rainfall-related causes of water storage deficit and other socioeconomic causes. These might include a decline in standards of infrastructure maintenance or loss of storage capacity due to reservoir siltation. We analyzed trends in seasonal rainfall excesses and deficits on the basis of normalized rainfall data and 3-year moving averages for four stations in the Vaigai watershed (Ramanathapuram, Kamadi, Vattanam, and Melur). Available records span 60–103 years (Figure 3b). This approach helps to capture rainfall variability for each station and to establish how the satellite image acquisition dates rank on the rainfall deficit scale provided by the z deviate scores. In this region, maximum reservoir levels should be expected around mid-January, i.e., just after the end of the rainy season. In order to test the capacity of remote sensing at detecting small to moderate variations in water stocks, we deliberately targeted rainfall years for which rainfall deviations from the long-term average were neither excessively positive nor excessively negative because there is little value in comparing full reservoirs (high-surplus year) with empty ones (drought

year). We will show that the method is sufficiently sensitive to detect small spatial and temporal changes.

[13] In summary, quantifying the variability of water stocks and tank-irrigated cropping areas between different dates helps to assess the relative impacts of climatic variability and human factors. Water stocks are expected to be positively correlated with seasonal rainfall and levels of collective involvement in infrastructure maintenance.

2.3. Image Processing

2.3.1. Preprocessing of the Landsat Series

[14] Eleven Landsat multispectral scanner (MSS), thematic mapper (TM), and Enhanced Thematic Mapper Plus (ETM+) georeferenced images covering the entire study area were selected (Figure 5) and calibrated to convert digital numbers to exoatmospheric reflectance. Given the registration dates of the MSS images (Figure 5) and their coincidence with a year of excess rainfall, these were chosen as the reference state for delimiting tank beds and assessing trends in land cover change and water stocks over time. We assumed from the regional literature that a very large majority of tanks at all registration dates were in use, with few renovation schemes between 1973 and 2001.

[15] MSS scenes consist of four bands corresponding to green and red in the visible spectrum ($0.5\text{--}0.6\ \mu\text{m}$, green and $0.6\text{--}0.7\ \mu\text{m}$, red) and to two connected bands in the near-infrared (NIR) spectrum ($0.7\text{--}0.8\ \mu\text{m}$ and $0.8\text{--}1.1\ \mu\text{m}$). TM images consist of seven channels, including three bands in the visible spectrum ($0.45\text{--}0.52\ \mu\text{m}$, blue; $0.52\text{--}0.6\ \mu\text{m}$, green; and $0.63\text{--}0.69\ \mu\text{m}$, red), one NIR band ($0.76\text{--}0.9\ \mu\text{m}$), one midinfrared (MIR) band ($1.55\text{--}1.75\ \mu\text{m}$), one short-wave infrared (SWIR) band ($2.08\text{--}2.35\ \mu\text{m}$), and one thermal infrared (TIR) band ($10.4\text{--}12.5\ \mu\text{m}$). In addition to

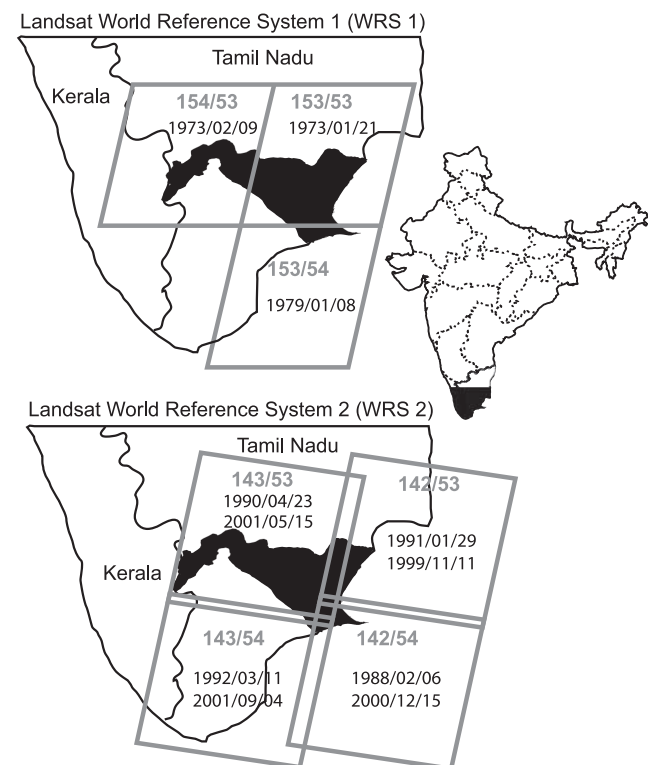


Figure 5. Coverage and acquisition dates of Landsat images used in the study.

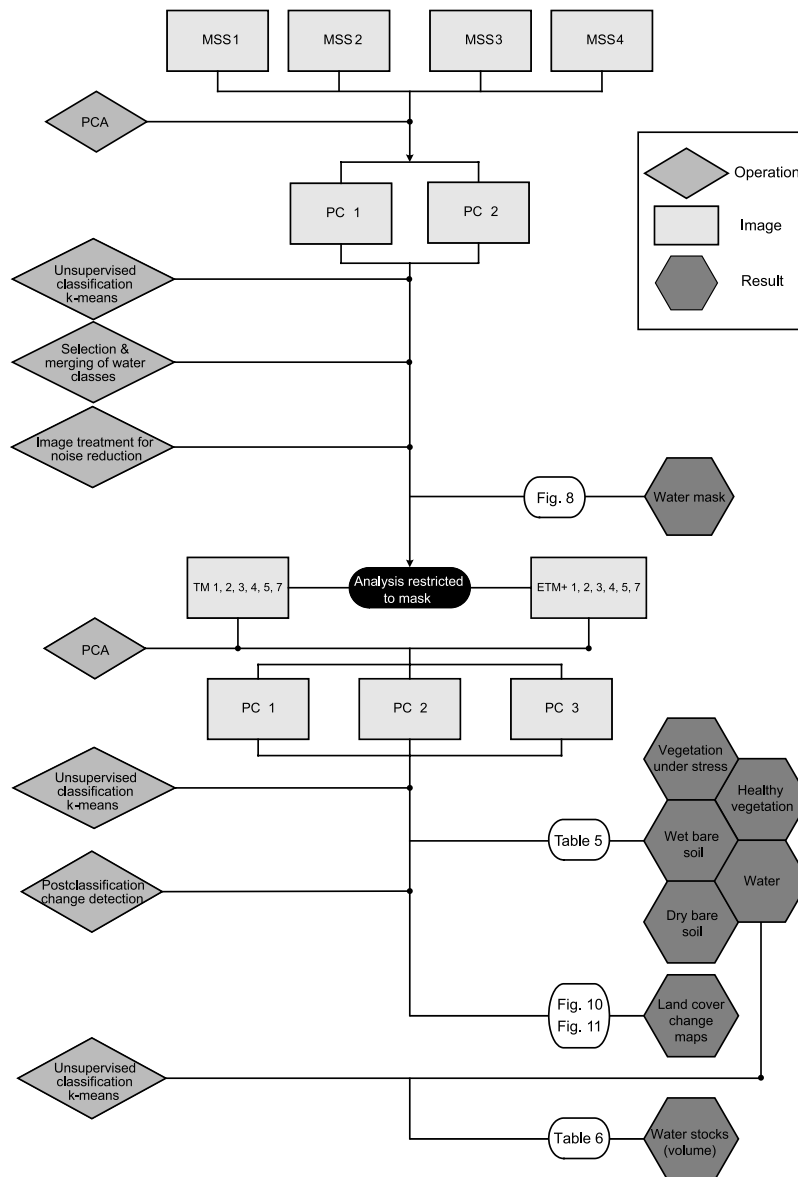


Figure 6. Flowchart summarizing methodology used in the study.

these, ETM+ images contain a 15-m spatial resolution panchromatic band (0.52–0.9 μm, panchromatic).

2.3.2. Detection of Aquatic Surfaces

[16] The sequence of data processing operations followed in this study is summarized in Figure 6. The flowchart can be used to follow through the steps described in the following sections. The detection of water surfaces by remote sensing is not a trivial exercise because open water presents a wide range of reflectance patterns determined by the interplay between surface, volume, and bottom reflectance values. These parameters are varyingly influenced by standing or floating vegetation, turbidity, dissolved matter, and algal content and affect the penetration of light. Furthermore, naturally blurred boundaries between soil, vegetation, and water make the extraction of water bodies from satellite scenes quite difficult.

[17] Several methods suitable for the detection of aquatic surfaces and the delineation of coastlines from remotely sensed images exist [Frazier and Page, 2000; Ouma and

Tateishi, 2006]. Three of these were applied here to the MSS images for comparative purposes. The first refers to a normalized difference water index (NDWI). The original NDWI needs to be obtained from NIR and MIR bands [Gao, 1996], but the MIR band is unavailable in MSS images. This, therefore, restricts the applicability of the technique to images that postdate the launch of Landsat TM. For that reason, we used a revised NDWI after Ouma and Tateishi [2006], which uses the green (G) and NIR bands in the equation $NDWI = (NIR - G)/(NIR + G)$. These two bands are available in the MSS images used here (bands 4 and 7). Because water presents higher reflectance values in the green band than in the NIR band, the index harnesses that sharp difference through the band ratio and is thus well suited to the detection of aquatic surfaces. To produce a binary mask for an image, class separation is performed by setting a low threshold on the obtained index (Table 1). This threshold was visually delimited using a false color composite image (red, MSS 7; green, MSS 5; and blue, MSS 4).

Table 1. Statistics Summarizing the Tank Detection Methods for MSS 153/53

	Methods		
	PCA	NDWI	Thresholding ^a
Threshold	na ^b	-0.97 to -0.69	0 to 0.05
Number of tanks detected	2312	2398	3169
Total water area, km ²	725	688	1019
<i>Mean Spectral Response (SD)^c</i>			
MSS 4	0.33 (0.09)	0.30 (0.10)	0.25 (0.09)
MSS 5	0.24 (0.08)	0.22 (0.09)	0.17 (0.08)
MSS 6	0.15 (0.06)	0.13 (0.06)	0.11 (0.04)
MSS 7	0.04 (0.02)	0.03 (0.01)	0.03 (0.01)
<i>Mean Spectral Response in Cloudy Area (SD)^c</i>			
MSS 4	0.32 (0.09)	0.29 (0.11)	0.19 (0.05)
MSS 5	0.24 (0.09)	0.21 (0.11)	0.12 (0.04)
MSS 6	0.15 (0.06)	0.13 (0.07)	0.10 (0.02)
MSS 7	0.04 (0.02)	0.04 (0.02)	0.04 (0.01)
<i>Mean Spectral Response of Image Differences (SD)^{c,d}</i>			
MSS 4	0.35 (0.05)	0.23 (0.12)	na ^b
MSS 5	0.28 (0.05)	0.16 (0.13)	na ^b
MSS 6	0.20 (0.04)	0.12 (0.09)	na ^b
MSS 7	0.07 (0.01)	0.04 (0.02)	na ^b

^aThresholding is for MSS 7.

^bNa, not applicable.

^cValues given are the mean followed by the standard deviation (SD) in parentheses.

^dTest zone 1 included in PCA procedure but not in NDWI. Test zone 2 included in NDWI procedure but not in PCA.

[18] The second method, hereafter called the threshold method, is also based on thresholding and involves setting a low threshold (Table 1) on MSS channel 7 (0.8–1.1 μm). Because of the strong absorbance of water bodies in this channel, it is a relevant way of distinguishing between wet and dry surface features [Frazier and Page, 2000].

[19] The third method is based on principal component analysis (PCA) computed from the four MSS channels followed by an unsupervised k means classification of the first resulting components. Contrary to the two previously mentioned methods, PCA is not specifically designed for the recognition of water bodies but remains a very general and efficient technique for the detection of features that exhibit weak radiometric contrast with their neighborhoods. The results of the PCA are the principal components, which lead to the extraction of new, decorrelated channels [Richards, 1999]. Given that the first few components contain most of the information present in the data, the remaining ones are ignored in subsequent pixel classification procedures (Figure 6). On the MSS images, the first two components generally contained more than 98% of the information. Concern with implementing an unsupervised classification was motivated by the aim to elaborate a general and replicable methodology based on automatic classification procedures applied to a vast geographic region. Therefore, no prior field work was tied to this analysis although interpretations used empirical knowledge acquired by the authors both in the field and through the literature.

[20] Binary images of aquatic surfaces were generated by each of the three methods described above for comparative purposes (Figure 7). The following stage consisted in

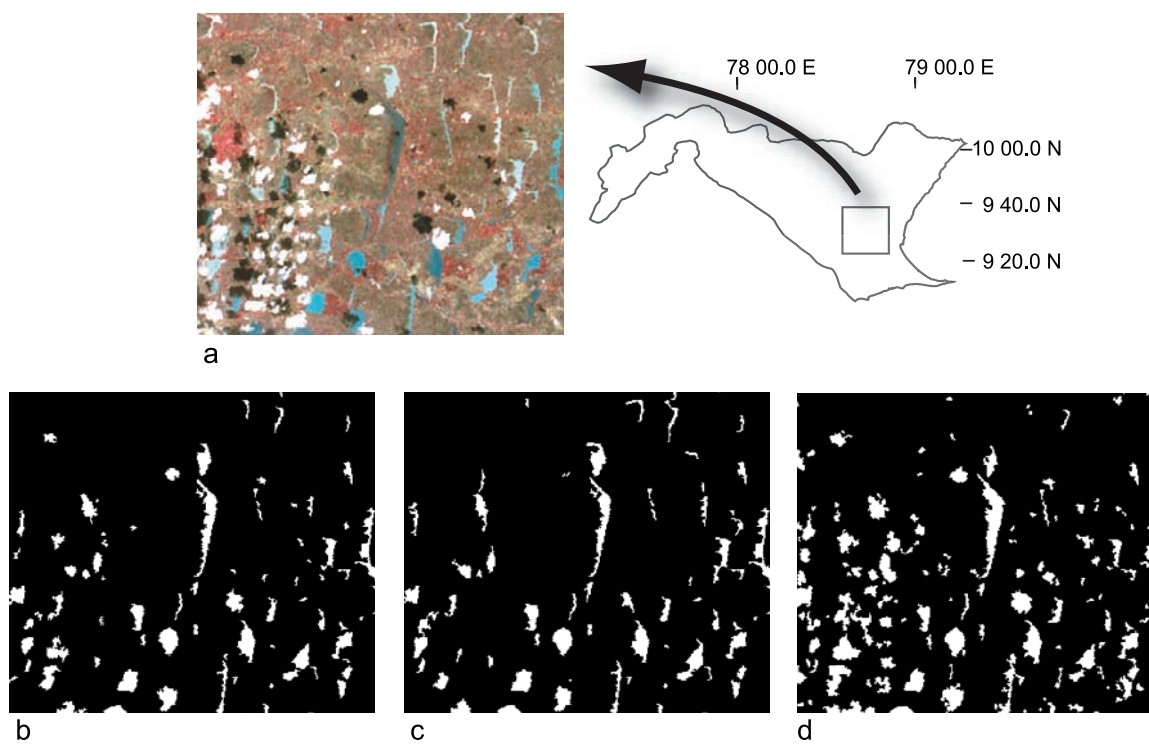


Figure 7. Sample of (a) initial MSS image illustrating comparative accuracy of the three automated procedures used to detect tanks beds. Resulting binary images display the (b) NDWI, (c) PCA, and (d) MSS 7 thresholding approaches. Note difference in surface area of cloud shadows and of thin, elongated tanks as an illustration of the relative behaviors of each method.

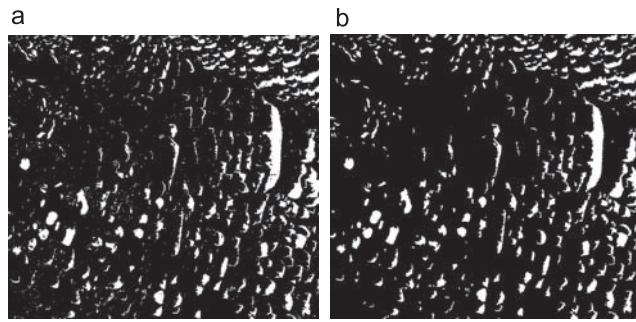


Figure 8. Binary images (a) before and (b) after noise removal by application of PCA and mathematical morphology procedures (see text).

eliminating from the binary images any small entities likely not to be tanks, such as natural depressions or flooded paddy fields. In order to avoid modifying the size and morphology of the tanks, a geodesic reconstruction [Serra, 1982] was performed in which the original image is first eroded and then reconstructed by successive geodesic dilations. A hole-filling transformation was subsequently carried out (Figure 8), which consists of filling entities that were counted out as nonaquatic because of local anomalies in the water body (aquatic vegetation, etc.) or because of pixel size but were necessarily part of the tank area because tanks rarely contain islands.

[21] The relative performances of the three pixel classification methods were evaluated by analysis of the means and standard deviations of their spectral responses in each MSS band. Validation was further backed up by visual analysis of the tanks seen in the false color composite of Figure 4. The most accurate image of tank water surfaces obtained was subsequently used as a mask of the tank beds and was vectorized for further analysis with the Landsat TM and ETM+ data (Figure 8b).

2.3.3. Detection of Land Mosaics Within the Tank Beds

[22] In order to determine the range of surface features within the areas defined as tank beds after MSS image processing, the entire set of Landsat TM and ETM+ was analyzed. A PCA followed by a k means classification in 10 classes was performed on pixel sets of the TM and ETM+ images contained within the masks previously obtained from the MSS classification. On the basis of its spectral signatures, each class was interpreted and recoded in one of five classes predefined for their relevance to land use and land cover change: dry bare soil, wet bare soil, water, healthy vegetation, and vegetation under stress. Classes presenting high spatial and spectral heterogeneity were merged and iteratively reclassified. Given the wide spectral window represented by these five classes, all pixels could be allocated to one of the categories. This simple and easily replicated classification was also suited to the goal of generating change detection maps.

2.3.4. Change Detection Procedure

[23] On the basis of the land surface classification, a change matrix was generated for some pairs of TM and ETM+ images corresponding to different dates. This data-merging technique allows so-called change detection maps to be generated, i.e., color-coded maps that display from-to categories of land cover change between two chosen dates.

Because it compares images that have already been classified, this procedure is relatively insensitive to variation in the spectral characteristics of objects between two dates, which makes it one of the most precise methods available for detecting surface changes [Mas, 1999]. Choice of similar registration dates was essential to maintain vegetation and hydrologic surface conditions as comparable as theoretically possible. For that reason, change detection was restricted to image pairs with small calendar offsets. This excluded TM and ETM+ scenes 143/54.

2.3.5. Quantification of Water Stocks

[24] Assessing the depths of water bodies is a difficult task because different factors contribute to modifying the spectral response. However, obtaining depths for individual tanks over a vast region through field surveys when no databases are available is even more impractical.

[25] In order to estimate water depths from satellite imagery, we chose a method based on a simple rule. Differences between the observed spectral response and the theoretical spectral signature of pure water are commonly generated by the interference between the surface, volume, and bottom reflectance of a water body. Accordingly, the critical parameter affecting the calculation of water volumes based on water depth estimates is the variability in spectral response of the tank bed. Given the radiometric properties of water, the variability of interest essentially concerns the visible spectrum and is predominantly controlled by soil color. Because the predominantly light-colored soils in the study area have a higher spectral response than water in the visible spectrum, the simple rule applied here is that water depth in a tank is inversely proportional to spectral response in the visible spectrum (see auxiliary material, Figures S1 and S2¹). Binary masks corresponding to the previously defined aquatic surfaces were generated for each image on this basis. An unsupervised classification of visible MSS, TM, and ETM+ bands based on the k means algorithm involving two classes (i.e., deeper and shallower water bodies) was performed within each mask across the entire regional mosaic.

[26] For obvious reasons, physical water depths could not be measured independently in the field on the image registration dates. This depth detection method is, therefore, inevitably relative in the sense that the attribution of water depth values to each class is a function of the spectral responses of the other classes. The method therefore provides maps of spatial variation in relative water depth. Additional accuracy in the classification of water depths, however, can be gained from empirical knowledge. The literature [e.g., Vaidyanathan, 2001] indicates that mean tank water depths in this part of Tamil Nadu rarely exceed 1.5 m. Even though tank design capacity is often larger, these depth values reflect capacity loss from decades of siltation and poor infrastructure maintenance. A mean total volume of water at any given time can thus be calculated from the scale of a single tank to that of an entire region.

[27] Here, as an example of what can be achieved, we divided the tank water surfaces into two depth classes, arbitrarily setting the mean of the shallower class at 0.50 m and that of deeper water bodies at 1.5 m. The tank

¹Auxiliary materials are available in the HTML. doi:10.1029/2007WR006065.

Table 2. Runoff Coefficient in Catchment Areas

	Clay	Clay Loam	Sandy Loam
Bare soil	0.7	0.6	0.4
Vegetation	0.5	0.4	0.2

areas classified as either deep or shallow on this basis were then multiplied by mean depth to obtain volumetric water stocks. In the case of the MSS images, the availability of comparable registration dates made it possible to calculate the total water stock for the entire study area. Meanwhile, for the TM and ETM+ images, which suffer from more significant offsets in registration dates, water volumes were calculated within the spatial limits defined by each individual scene. The accuracy of calculations is obviously highly dependent on the availability of tank depth databases, but emphasis here is chiefly on methodology. Values can be adjusted as data sources improve in user-defined areas of interest.

2.3.6. Implementation of a Regional Water Balance as an Independent Test

[28] In order to independently test the accuracy of water stock evaluation by remote sensing, we attempted a summary regional water balance in a GIS for the 1972 and 1978 rainy seasons that immediately preceded the MSS acquisition dates. Water balance equations for a catchment are commonly given as $P = (QR) + E \pm \Delta V$, where P is precipitation, Q is runoff, R is a runoff coefficient ($0 \leq R \leq 1$), E is total evapotranspiration loss, and V represents storage. Tank water stocks on the registration dates were calculated by considering that $V_t = P_t - (E_t + S_t)$, where V_t is water volume, P_t is rainfall over the tank surface, E_t is evaporation of the tank water, and S_t is seepage loss.

[29] A precipitation map was prepared by nearest-neighbor interpolation of data known for 10 rainfall stations. The catchment area for all tanks was also estimated. Given the low-gradient topography of the plain, it proved impossible to reliably establish microcatchment boundaries from digital elevation models such as the Shuttle Radar

Topography Mission (90-m resolution) because flow grid algorithms perform poorly on flat topography at that resolution. Instead, a buffer zone mimicking the catchment areas was drawn around the tanks in the GIS. Buffer radius, r (m), was set to be proportional to tank surface area, A (m^2). Using the ad hoc formula $r = kA$, the aggregate buffer area obtained with $k = 10^{-3}$ (m^{-1}) provided a value of 3496 km^2 for a total tank water surface area of 855 km^2 , i.e., a catchment-to-tank surface area ratio of 1:4. This is in broad agreement with empirical evidence for the region. Although for technical reasons the buffers do not strictly coincide with the true geographic boundaries of the catchment areas, the practical adequacy of observing a realistic catchment-to-tank surface area ratio is sufficient for the purpose of establishing a simple water balance at this regional scale. Furthermore, the buffer approach is consistent with evidence that closely spaced tanks form tank groups that collectively share a vast, continuous catchment area [Mosse, 2003]. In those areas, double counting of buffers was avoided.

[30] In order to incorporate runoff coefficients into the water balance, two vector layers were generated in the GIS for land cover and soil texture, respectively. Land cover classes were calculated on the basis of a normalized vegetation index (NDVI) defined as $NDVI = (MSS\ 6\ minus\ MSS\ 5)/(MSS\ 6\ plus\ MSS\ 5)$. An NDVI threshold set on +0.3 adequately distinguished between bare soil (<0.3) and vegetated areas (>0.3). Soil texture was obtained by digitizing and georeferencing the 1:500,000 Soil resource map of Tamil Nadu [Natarajan *et al.*, 1996]. Three texture classes defined as clay, clay loam, and sandy loam were extracted on the basis of exhaustive inventories provided by Natarajan *et al.* [1996] and were attributed to the runoff coefficients commonly recommended for Indian soil conditions [e.g., Tideman, 1996]. Polygon overlay and intersection produced six runoff classes (Table 2).

[31] P_t was obtained by multiplying the tank surface areas by rainfall depths as provided by the interpolated rainfall map. For evaporation and seepage, data available for tanks in Sri Lanka under climatically similar conditions were used [Jayatilaka *et al.*, 2003]. Daily evaporation rates are 4–

Table 3. Regional Water Balance for the Rainy Seasons Preceding Capture of MSS 153/53 and 154/53

	Sep	Oct	Nov	Dec	15 Jan
	<i>Inputs^a</i>				
Rain on tank, m^3	84,704,076	358,781,641	151,440,273	161,144,956	0
Runoff, m^3	171,652,617	724,174,710	327,955,947	354,575,372	0
	<i>Losses^a</i>				
Evaporation, m^3					
6 $mm\ d^{-1}$	153,987,495				
5 $mm\ d^{-1}$		128,322,913			64,161,456
4 $mm\ d^{-1}$			102,658,330	102,658,330	
Infiltration, ^b m^3	51,184,599 (50)	251,454,509 (25)	226,220,283 (20)	263,588,626 (20)	247,548,262 (25)
Water balance at end of month, m^3	51,184,599	754,363,528	904,881,134	1,054,354,506	742,644,787

^aAs commonly observed, the tanks are considered totally empty at the beginning of September. To obtain water volumes, the reference tank area used was the aquatic surface area measured on the MSS image registration dates. This is an approximation inasmuch as it overlooks the growth of water surface area between September and January, which is unknown but would affect infiltration and evaporation because these are some functions of surface area. Magnitudes of inaccuracy related to this will depend on the form of the depth-to-area curve over time, with smallest error if tank area grows much faster than tank depth.

^bInfiltration is calculated as daily rate (given in parentheses) multiplied by 30 d on the basis of data provided by Jayatilaka *et al.* [2003]. Values decline as a function of temperature with the cooler months.

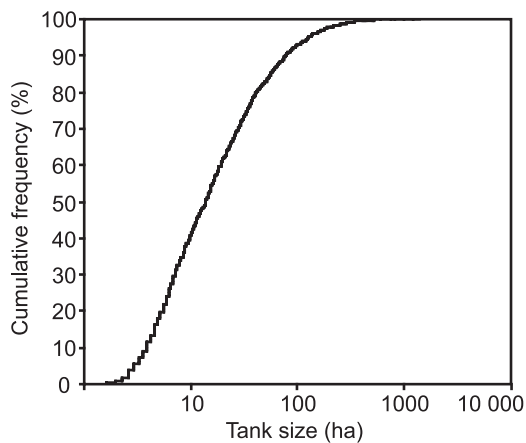


Figure 9. Cumulative distribution of tank sizes across study area as detected after PCA classification on the MSS images.

6 mm depending on the month, and monthly seepage losses occur at rates of 20–50% of the water stock (Table 3).

3. Results

3.1. Comparison Between Image Processing Methods

[32] In order to determine the most accurate method of tank detection, we performed a comparison between the binary images produced by each of the three water detection methods described in section 2.3.2. Tests were deliberately performed on the MSS 153/53 image because it not only presented signs of heterogeneity in water body spectral responses but also exhibited some cloud cover in its southwest corner. Because of the common occurrence of clouds in tropical settings and the potential for mistaking cloud shadows for water surfaces due to an overlap in spectral response patterns, it seemed useful to test the capacity of reservoir detection methods to avoid confusion with cloud shadows. After removal of noise by geodesic operations (see section 2.3.2), an analysis of spectral signatures backed up by visual analysis allowed a comparison to be drawn between each of the three methods. Table 1 shows that means of the spectral response values obtained with the PCA and NDWI methods for the entire image were very similar in all the bands. Moreover, the ranges defined by these two methods match well with the outlines of different water bodies identified visually as tanks on a false color composite of MSS 153/53. In contrast, the threshold method presented lower values of means in the first three bands. This indicates that this method does not detect shallower water bodies located on brighter soils because these soil types increase the spectral responses in all MSS bands, and particularly in MSS 7, which is the discriminating channel for such surface features. Thresholding also tended to classify as aquatic surfaces wet dark soils that have a low spectral response in MSS 7, thereby artificially overestimating the extent of tank areas (see Table 1). Mean values obtained for the cloudy area only reinforced this bias.

[33] The other two methods produced much closer means, but the NDWI generated higher standard deviation. Standard deviation analysis provides information on levels of class heterogeneity. For a more accurate comparison, we excluded the geographic overlap areas between images and

computed mean and standard deviation values for areas classified by only one method at a time (representing 8.41 km² for the PCA method and 7.01 km² for the NDWI method; see Table 1). The NDWI showed not only higher standard deviation values but also lower means, indicating the relative inability to filter out some cloud shadows. The PCA produced slightly higher means than in the previous experiment because the radiance of lateritic soils present in the cloudy areas increased reflectance values. However, PCA also generated lower standard deviation values, thus implying a greater homogeneity in spectral responses.

[34] In summary, although the NDWI method seems well suited to the detection of water bodies in cloud-free zones, its performance is challenged in the presence of cloud shadows. Thresholding of MSS 7 proved suitable for detecting water pixels but, in agreement with caveats formulated by *Frazier and Page* [2000], tended to include a relatively high proportion of pixels that did not belong to water bodies. Ultimately, even though some pixels remained misclassified, the PCA method performed best in distinguishing cloud shadows from water surfaces (as seen in Figures 4 and 7). Table 1 also shows that both the PCA and NDWI methods provide more conservative estimates of water surface areas than the threshold method. This is important because the risk of overestimating water reserves as a consequence of artifacts in data processing is detrimental to the precautionary requirements of water resource management, forecasting, and planning (compare Figures 7b, 7c, and 7d). Because of its all-around stability, accuracy, mathematical transparency, and replicability, the PCA method came out as the most recommendable for the detection of water surfaces based on reflectance values and was preferred in the subsequent steps of the change detection procedure.

3.2. Water Resources

3.2.1. Detection of Reservoir Beds

[35] Out of the 11,310 km² of the total study area, tanks cover 7.6% of the land surface. In general, it is established that in south India the ratio between tank command area and water spread area is close to 1 [*Mosse*, 1997]. It can therefore be estimated that the tank-irrigated area during the 1970s was ~85,500 ha, so the area devoted to tanks and their irrigated perimeters was ~15% of the total land area. However, given the spatial heterogeneity in tank size, the cumulative distribution of tanks is not linear (Figure 9). Table 4 shows in detail that large tanks (>100 ha) make up 44% of the total water storage area despite representing just 7% of the total number of reservoirs. In contrast, small tanks (<10 ha) make up 41% of the total number of reservoirs but only concern 7% of the land area devoted to water storage.

Table 4. Spatial Attributes of Tanks on MSS Images

Tank Size, ha	Number of Tanks	Total Water Surface Area, km ²	Relative Water Surface Area, %
<10	1017	57	7
10–100	1297	419	49
>100	180	379	44
Total	2494	855	100

Table 5. Surface Features of Tank Beds on Paired Dates

Scene	Number of Months After or Before End of Monsoon ^a	Year	Surface Features, %					Total
			Vegetation		Bare Soil		Water	
			Under Stress	Healthy	Dry	Wet		
142/53	+1	1991	6.3	5.4	41.3	14.5	32.5	100
	-1.75	1999	21.5	23.3	14	10	31.2	100
142/54	+1	1988	11.3	13.4	7.2	45.1	23	100
	-0.5	2000	17.2	12.3	22.2	36.8	11.5	100
143/53	+3.75	1990	18.4	6.6	17.6	52.5	4.9	100
	+4.5	2001	11.1	7.4	33.4	38.4	9.7	100

^aMonths after are represented by plus signs, and months before are represented by minus signs.

3.2.2. Surface Features in Tank Beds From Landsat TM and ETM+ Images

[36] Among the five land surface categories defined in section 2.3.3, healthy vegetation is defined by high reflectance values in the NIR and low reflectance values in the MIR (see auxiliary material, Figure S2). It typifies plants during their growth seasons, a time when they also exhibit a relatively broad surface area. This category corresponds to (1) grassy cover colonizing exposed tank beds, (2) irrigated crop encroachment onto the tank bed, and/or (3) trees planted on tank foreshores as a component of social forestry programs. The presence of healthy vegetation during the dry season, for instance, indicates some form of agricultural land use. Distinction between these categories would require greater pixel resolution than is provided by the images used, but high-resolution imagery such as that provided by Google Earth confirms that all three of these situations exist.

[37] Vegetation under stress contrasts with healthy vegetation by subdued reflectance values in the NIR and higher values in the MIR (see auxiliary material, Figure S2). It would correspond to woody or herbaceous plants in the process of aging or desiccation. Ground cover in such areas is incomplete, and the spectral response is thus blurred by the exposure of bare soil. In any season, the presence of this

land use category suggests at least temporarily limited tank use or maintenance.

[38] Dry bare soil is characterized by high reflectance in both the visible and IR spectra (see auxiliary material, Figure S2) and indicates prolonged empty tank conditions. MIR values are critical in the appraisal of humidity because MIR corresponds to a band of almost complete water absorption. Wet bare soil differs from dry soil by lower reflectance values in the visible and MIR bands (see auxiliary material, Figure S2) and describes varying states of saturation depending on soil texture and field capacity.

[39] Table 5 provides synoptic quantitative information on change in tank bed features over time. Given that scene 142/53 (1999) was acquired before the end of the rainy season, the difference in aquatic area between 1991 and 1999 does not indicate a decrease in the primary function of the tanks. Scenes corresponding to 143/53 were acquired during the dry season and are therefore of little use in assessing postmonsoon water levels. Finally, differences between the two images of scene 142/53 are minimal and are chiefly explained by rainfall totals (see Table 5). At this scale, the maximum relative aquatic surface area obtained from the images was ~32.5% (on TM 142/53). It can be inferred that the principal period of decline in tank water

		Initial State: 1991 (TM 142/53)				
		Water	Wet bare soil	Vegetation Under stress	Healthy vegetation	Dry bare soil
		(%)	(%)	(%)	(%)	(%)
Final state: 1999 (ETM+ 142/53)	Unclassified	1.2	1.3	0.8	1.2	1.2
	Water	50	32.7	12	7.6	20.6
	Wet bare soil	9.7	13.3	8.9	8.1	9
	Vegetation Under stress	14.5	20.1	27.3	24	24.8
	Healthy vegetation	15.7	24.4	46.5	54	19.3
	Dry bare soil	7.3	6.8	2.1	2.9	24.6
	Clouds	1.5	1.3	2.4	2.3	0.7
	Class Total	100	100	100	100	100
	Class Changes	49.9	86.7	72.7	46.1	75.4
	Image Difference	-5.1	-31.7	+245.7	+328.3	-66.4

Figure 10. Change detection matrix of surface features (1991–1999) on scene 142/53. Class changes is the percentage of the initial class that evolved toward a different surface feature. Image difference is the evolution of a surface feature over the entire image area between initial and final state and is expressed in percent.

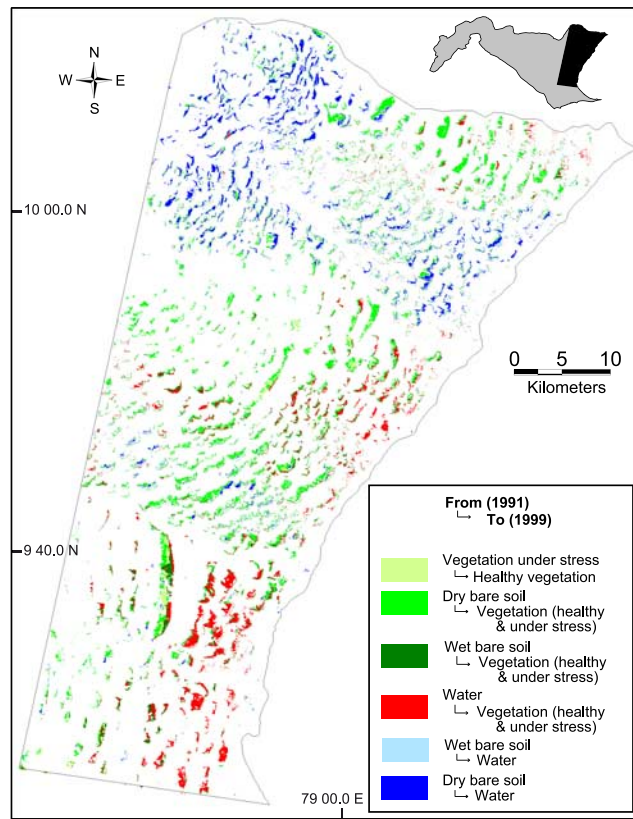


Figure 11. Change detection map of tank beds on scene 142/53 between 1991 and 1999. Area is identical to that displayed in Figure 4.

storage occurred between the 1970s and early 1990s. Most of the decrease observed between the early and late 1990s can be explained by monsoon variability. Nevertheless, other surface features, particularly vegetation, remain good proxies for assessing the challenges facing tanks as water storage devices.

3.2.3. Change Detection of Soil Surface Features Within Tank Beds

[40] Change statistics are compiled in Figure 10. They describe detected changes in surface features on tank beds within each of the five previously defined land cover classes (see section 2.3.3). Twenty $((5 \times 5) - 5)$ dynamic classes were thus generated. The accuracy of this change detection method is clearly a function of the quality of the classification method previously carried out.

[41] Change detection maps are one of the key outputs of multitemporal image analysis. However, the large number of change detection classes is restricted here to relatively small surface areas, i.e., tank beds, and therefore raises problems of visual representation. Two approaches were possible in this respect. One would have been to produce detection maps restricted to one class at a time. Collectively, the maps would have contained all the information but would have remained unattractive. The other method, used here, attempts to display on a single map the quantitatively most significant changes alongside changes that are deemed qualitatively unique or unexpected (Figure 11). The number of change classes is therefore much reduced, and the map output is more intelligible.

[42] In Figure 11, all classes represent from-to changes exceeding 20% of the initial state. Both of the vegetation classes were clustered because the presence of either category in a tank bed reflects a relative decline in the primary function of the tank, i.e., water storage. Not only does the change detection matrix (Figure 10) highlight a net increase in vegetation cover (vegetation under stress, +245% and healthy vegetation, +328%), mainly at the expense of bare soil (wet, -31% and dry, -66%), but the map additionally indicates that vegetation shows little sign of recession wherever it had already established itself in 1991. In this particular example, also note from Figure 10 that total aquatic surface areas have only fallen by 5% between the two dates. However, the map shows that the spatial distribution of aquatic surfaces has changed. Together, these indications suggest that the observed change in spatial patterns may have more to do with land use and social parameters than with rainfall. Figure 11 highlights a contrast between three distinct zones: in the south, areas either previously flooded or exhibiting bare soil in 1991 were vegetated in 1999; in the center, bare soil in 1991 had become vegetated in 1999; and in the north, aquatic surfaces during the same period increased over exposed bare soil.

[43] The detected progression of vegetation in tank beds that were flooded in 1973 was independently confirmed by the computation of an NDVI. The difference between the initial (1991) and final (1999) indices produces a map (see auxiliary material, Figure S3) that reveals a net increase in biomass in several areas of the image but most conspicuously within the tank beds. Mapping changes in surface features reveals local dynamics, spatial discontinuities, and homogeneous small areas. All of these are useful to water resources research because they may reflect common cultural values, agricultural practices, or ecological adaptations.

3.2.4. Estimation of Water Stocks by Remote Sensing

[44] Overall, within the uncertainty limits of the synoptic method employed, the 1973 mean total volume of tank water (obtained as the averaged sum of class means) stored in the study area at the end of the rainy season was $846 \times 10^6 \text{ m}^3$, representing an average tank depth of $\sim 0.88 \text{ m}$. Given the characteristics of the 1972 and 1978 rainfall years, this value is an estimate of the basin's potential for tank irrigation at above-average tank capacity. Below we illustrate the kind of additional information that can be extracted from the approach presented.

[45] Certain water stock values are directly comparable (Table 6). For instance, compared to the situation on 21 January 1973, water stocks on 29 January 1991 were reduced by 0.277 km^3 because of a relative rainfall deficit having occurred in late 1990. A paddy crop in Tamil Nadu requires $\sim 1200 \text{ mm}$ of water [Gourou, 2000], and seasonal consumptive use for other crops can be calculated in this way on the basis of the widely used Blaney-Criddle method [Blaney and Criddle, 1962]. By extrapolation, the deficit in tank water for 1991 implies a reduction in tank-irrigated paddy crops of 23,083 ha out of the 253,300 ha total for scene 142/53. Such deficit situations would call for some compensatory mechanism from irrigation sources other than tanks. A relative water deficit also occurred in 1999, with a calculated volume loss of 0.050 km^3 compared to 1991. Note, however, that the 11 November 1999 registration date falls only halfway through the rainy season.

Table 6. Volumetric Water Stocks in the Tanks of the Study Area on Different Dates^a

Scene (World Reference System 2)	Sensor	Date	Seasonal Rain Already Fallen on Image Acquisition Date, mm	Number of Months After and Before the End of the Monsoon Season ^b	Mean Volume, 10 ⁶ m ³
142/53	MSS	21 Jan 1973	575	+0.75	460
	TM	29 Jan 1991	555	+1	183
	ETM+	11 Nov 1999	335	-1.75	133
143/53	MSS	21 Jan 1973 and 8 Jan 1979	682	+0.25 and +0.75	686
	TM	23 April 1990		+3.75	33
	ETM+	15 May 2001		+4.5	38
142/54	MSS	21 Jan 1973 and 29 Jan 1979	682	+0.25 and +0.75	103
	TM	6 Feb 1988	763	+1	29
	ETM+	15 Dec 2000	549	-0.5	11

^aRainfall stations used are Ramanathapuram (scene 142/53), Melur-Kamadi (scene 143/53), and Ramanathapuram-Vattanam (scene 142/54). Mean seasonal rainfall (October to December) for Ramanathapuram (1941–2000), 578 mm; Melur (1901–2004), 411 mm; Vattanam (1941–2000), 500 mm; and Kamadi (1941–2000), 375 mm.

^bMonths after are represented by plus signs, and months before are represented by minus signs.

[46] For scene 143/53, only surface water resources for 1990 and 2001 are comparable week for week. The relatively higher water levels in 2001 reflect an upturn in rainfall after a prolonged period of relative deficit during the 1990s. However, the presence of tank water in April, i.e., 4 months after the rainy season but also soon after the secondary rainfall peak that normally occurs around that time (see Figure 3a), could be the result of an efficient management of the tank system and its water resources. The water-filled tanks during this season are small. Such size-related heterogeneity indicates that smaller tanks are more efficient than larger reservoirs at storing runoff associated with limited rainfall episodes such as this springtime rainfall peak. This advantage is likely related to smaller runoff concentration times in small catchments.

[47] With only a small offset in anniversary dates, the three images corresponding to scene 142/54 can also undergo comparison. Despite comparable rainfall settings in 1988 and 2000, a 72% difference and an 89% difference in water stocks are observed between the 1973 reference values and those of 1988 and 2000, respectively. Such a sharp difference could, for instance, be interpreted as a decline and express growing disaffection among farming communities for tank irrigation, accompanied by infrastructural degradation, a related decline in tank storage capacity, and a corresponding reliance on private bore well irrigation.

[48] In summary, the tentative socioeconomic interpretations given here are predicated on the widely documented basis that social disaffection for tank maintenance has grown over the last few decades. Clearly, at least in theory, alternative explanations could be hypothesized: for instance, different rules of water use between communities could explain some of the observed variability in water stocks at a given date. Ultimately, the accuracy of any of these interpretations requires testing with ground surveys, but the purpose of this essentially methodological study is to show the value of remote sensing as a tool in water resources research for outlining working hypotheses, mapping geographic anomalies, detecting potential problem areas, and designing field surveys more efficiently.

3.2.5. Estimation of Water Stocks by the Water Balance Approach

[49] The water balance approach (Table 3) yielded a water stock of $\sim 0.743 \text{ km}^3$, which differs from the remote sensing-based calculation by $\sim 0.104 \text{ km}^3$. Despite the

sensitivity of the water balance model to input parameter values such as buffer size (i.e., catchment-to-tank size ratio), runoff coefficient, or evaporation and seepage rates, the results obtained independently by those two water accounting methods are therefore of the same order of magnitude and suggest reasonable accuracy.

4. Discussion

[50] The remote sensing procedure chiefly requires an identification of parameters causing variations in spectral response as a function of water depth. Relative depth mapping is only possible because Indian tanks are relatively shallow water bodies. It would not work for water depths exceeding a few meters, which also means that in the case of tanks, error margins are limited; that is, there is a ceiling on error that prevents water stock estimates from being absurdly inaccurate. As such, the remote sensing approach appears to be easier to implement than a water balance method because it involves the acquisition of a smaller number of parameters from independent sources. The risk of error propagation in subsequent calculations is therefore also probably smaller.

[51] Precision on water stock calculations is partly related to the intrinsic limitations of satellite imagery for calculating aquatic surface areas. Regarding spatial resolution, for instance, some pixels located at the tank edge with MSS are likely to have been wrongly detected as either water or soil with the consequence of overestimating or underestimating tank area. Very small water bodies could also be missed, although in south India, reservoirs below the detection threshold of Landsat MSS and TM are dedicated to drinking water storage and therefore are irrelevant to this study. Another difficulty is that satellite imagery will not easily distinguish system tanks from nonsystem tanks without independent knowledge and may thus mistake some rain-fed tanks (which, however, represent an overwhelming majority) for river-fed reservoirs. Nevertheless, it remains possible to increase image resolution by using other satellite sources, and future tests should be able to constrain the magnitude of these imprecisions. A trade-off, however, between the higher resolution of recent satellite sensors and the historical time depth provided by the older MSS Landsat data is inevitable.

[52] Likewise, temporal resolution can be increased by using closely spaced pass dates, for instance, over the

Table 7. Synthesis of Land Use Dynamics in Tank Beds Detected Between 1973 and 2001

Process	Land Use in Tank Bed	Socioeconomic Interpretation ^a
Steady water storage capacity	High priority attached to water conservation	Collective tank maintenance upheld, social cohesion
Encroachment by herbaceous vegetation	Low priority attached to water conservation, reduced storage	Disaffection for tank irrigation, overtaken by groundwater irrigation
Lasting colonization by woody vegetation and other land uses	Low priority attached to water conservation; social forestry, agriculture, and buildings in tank bed	Decline of the tank as an irrigation tool, diversification of land use in tank bed

^aThe socioeconomic interpretation is hypothetical.

course of a cropping season. This could even provide the basis for a movie of tank water depletion over time and would be a way of detecting geographic patterns of asynchronicity in water release practices, possibly revealing variability in social rules. A denser grid of rainfall stations and water depth databases made available by appropriate authorities would also be desirable because this ultimately determines the calculation of the key parameter of interest, namely, water volumes.

[53] In summary, despite scope for improved calibration of quantitative results against higher-resolution data, this pilot study has brought out sharp subregional contrasts in terms of water resource potential and change in water-harvesting conditions over time. Table 7 summarizes the main evolutionary trends observed. The proposed approach is a step toward helping water management authorities on the ground to collect and compile data that will be relevant to the improvement of the remote sensing–based approach we advocate.

[54] Tank rehabilitation is only one of the possible solutions toward improving sustainable water resource management in south India. However, because of ongoing groundwater mining and high rainfall variability, tank upkeep is more than just an optional fallback. Lasting changes detected in the surface features of tank beds reflect local changes in village socioeconomic life that call for ground investigation and the possible implementation of appropriate policies or incentives. The synoptic appraisal of water-harvesting infrastructures may also assist in planning new structures for suitable land systems in other semiarid regions of the world [e.g., *Tauer and Humborg*, 1993]. Water harvesting structures similar to Indian tanks, although not always functionally or structurally identical, exist, for instance, in parts of northeast Brazil, Ghana, Sri Lanka, Sudan, Thailand, and northern India [e.g., *Prinz*, 1996; *Thiruvengadachari and Sakthivadivel*, 1997; *Barrow*, 1999; *Antonino et al.*, 2005; *Liebe et al.*, 2005].

5. Conclusion

[55] The synoptic, multispectral, multiresolution, and multirate approach developed in this study serves the purpose of establishing regional water resource inventories. It also assists in mapping spatial heterogeneities in water stocks and land use detected over user-defined time intervals. Results have suggested that climatic variability may not be the only cause of fluctuating water levels. Contrasts in the evolution of nonaquatic surface features within the confines of reservoir beds were shown to be potentially useful indicators of tank system degradation and economic performance. As such, remote sensing and GIS integration

provide powerful tools for building hypotheses and for crafting efficient field surveys designed to investigate how institutional, social, or economic factors affect the relationship between local populations and their water resources. Among available methods of water detection in remote sensing, unsupervised pixel classification based on PCA appears to generate the most stable and accurate results in most respects. It is replicable and can therefore easily be tested in other settings where decision making in integrated rural management is a priority.

[56] **Acknowledgments.** We appreciated the thorough and challenging reviews from Hugh Turrall, Associate Editor Steve Margulis, and two anonymous individuals, who contributed to improving the quality of this manuscript.

References

- Ambast, S. K., A. K. Keshari, and A. K. Gosain (2002), Satellite remote sensing to support management of irrigation systems: Concepts and approaches, *Irrig. Drain.*, *51*, 25–39, doi:10.1002/ird.26.
- Anbumozhi, V., K. Matsumoto, and E. Yamaji (2001), Towards improved performance of irrigation tanks in semi-arid regions of India: Modernization opportunities and challenges, *Irrig. Drain. Syst.*, *15*, 293–309, doi:10.1023/A:1014420822465.
- Antonino, A. C. D., C. Hammecker, S. M. L. G. Montenegro, A. M. Netto, R. Angulo-Jaramillo, and A. A. B. O. Lira (2005), Subirrigation of land bordering small reservoirs in the semi-arid region in the Northeast of Brazil: Monitoring and water balance, *Agric. Water Manage.*, *73*, 131–147, doi:10.1016/j.agwat.2004.10.001.
- Balasubramanian, R., and K. N. Selvaraj (2003), Poverty, private property and common pool resource management: The case of irrigation tanks in south India, *Working Pap. 2-03*, 61 pp., S. Asian Network for Dev. and Environ. Econ., Kathmandu.
- Barrow, C. J. (1999), *Alternative Irrigation: The Promise of Runoff Agriculture*, 172 pp., Earthscan, London.
- Blaney, H. F., and W. D. Criddle (1962), Determining consumptive use and irrigation water requirements, *Tech. Bull. 1275*, Agric. Res. Serv., U.S. Dep. Of Agric., Washington, D. C.
- Frazier, P. S., and K. J. Page (2000), Water body detection and delineation with Landsat TM data, *Photogramm. Eng. Remote Sens.*, *66*, 1461–1467.
- Gao, B. C. (1996), NDWI: A normalized difference water index for remote sensing of vegetation liquid water from space, *Remote Sens. Environ.*, *58*, 257–266, doi:10.1016/S0034-4257(96)00067-3.
- Gourou, P. (2000), *Riz et Civilisation* (in French), 299 pp., Fayard, Paris.
- Gunnell, Y., and K. Anupama (2003), Past and present status of runoff harvesting systems in dryland peninsular India: A critical review, *Ambio*, *32*, 320–324, doi:10.1639/0044-7447(2003)032[0320:PAPSOR]2.0.CO;2.
- Gunnell, Y., K. Anupama, and B. Sultan (2007), Response of the south Indian runoff-harvesting civilization to northeast monsoon rainfall variability during the last 2000 years: Instrumental records and indirect evidence, *Holocene*, *17*, 207–215, doi:10.1177/0959683607075835.
- Jayatilaka, C. J., R. Sakthivadivel, Y. Shinogi, I. W. Makin, and P. Witharana (2003), A simple water balance modelling approach for determining water availability in an irrigation tank cascade system, *J. Hydrol.*, *273*, 81–102, doi:10.1016/S0022-1694(02)00360-8.
- Kajisa, K., K. Palanisami, and T. Sakurai (2004), Declines in the collective management of tank irrigation and their impact on income distribution and poverty in Tamil Nadu, India, *Discuss. Pap. Ser. Int. Dev. Strategies 2004-08-005*, 29 pp., Found. for Adv. Stud. on Int. Dev., Tokyo.

- Li, Q., and J. Gowing (2005), A daily water balance modelling approach for simulating performance of tank-based irrigation systems, *Water Resour. Manage.*, 19, 211–233, doi:10.1007/s11269-005-2702-9.
- Liebe, J., N. van de Giesen, and M. Andreini (2005), Estimation of small reservoir storage capacities in a semi-arid environment: A case study in the Upper East region of Ghana, *Phys. Chem. Earth*, 30, 448–454.
- Mas, J.-F. (1999), Monitoring land-cover changes: A comparison of change detection techniques, *Int. J. Remote Sens.*, 20, 139–152, doi:10.1080/014311699213659.
- Mosse, D. (1997), Ecological zones and culture of collective action: The history and social organization of a tank irrigation system in Tamil Nadu, *S. Indian Stud.*, 3, 1–88.
- Mosse, D. (2003), *The Rule of Water: Statecraft, Ecology and Collective Action in South India*, 337 pp., Oxford Univ. Press, New Delhi.
- Natarajan, A., P. S. A. Reddy, A. D. Mosi, and J. Sehgal (Eds.) (1996), Soil resource map of Tamil Nadu, *Map 9*, 4 sheets, 1:500,000, Natl. Bur. of Soil Surv. and Land Use Plann., Nagpur, India.
- Ouma, Y. O., and R. Tateishi (2006), A water index for rapid mapping of shoreline changes of five East African Rift Valley lakes: An empirical analysis using Landsat TM and ETM+ data, *Int. J. Remote Sens.*, 27, 3153–3181, doi:10.1080/01431160500309934.
- Palanisami, K., and K. W. Easter (1987), Small-scale surface (tank) irrigation in Asia, *Water Resour. Res.*, 23, 774–780, doi:10.1029/WR023i005p00774.
- Palanisami, K., and R. Meinzen-Dick (2001), Tank performance and multiple uses in Tamil Nadu, south India, *Irrig. Drain. Syst.*, 15, 173–195, doi:10.1023/A:1012927722965.
- Prasad, K. S. S., S. Gopi, and R. S. Rao (1993), Watershed prioritisation using remote sensing techniques—A case study of the Mahbubnagar district, Andhra Pradesh, India, *Int. J. Remote Sens.*, 14, 3239–3247, doi:10.1080/01431169308904438.
- Prinz, D. (1996), Water harvesting: Past and future, in *Sustainability of Irrigated Agriculture*, edited by L. S. Pereira, pp. 135–144, A. A. Balkema, Rotterdam, Netherlands.
- Ranganathan, C. R., and K. Palanisami (2004), Modelling economics of conjunctive surface and groundwater irrigation systems, *Irrig. Drain. Syst.*, 18, 127–143, doi:10.1023/B:IRRI.0000040251.52864.7e.
- Rao, R. S., M. Venkataswamy, C. Mastan Rao, and G. V. A. Rama Krishna (1993), Identification of overdeveloped zones of ground water and the location of rainwater harvesting structures using an integrated remote sensing based approach—A case study in part of the Anantapur district, Andhra Pradesh, India, *Int. J. Remote Sens.*, 14, 3231–3237, doi:10.1080/01431169308904437.
- Rao, V. V., and A. K. Chakraborti (2000), Water balance study and conjunctive water use planning in an irrigation canal command area: A remote sensing perspective, *Int. J. Remote Sens.*, 21, 3227–3238, doi:10.1080/014311600750019859.
- Richards, J. A. (1999), *Remote Sensing Digital Image Analysis: An Introduction*, 240 pp., Springer, Berlin.
- Sakurai, T., and K. Palanisami (2001), Tank irrigation management as a local common property: The case of Tamil Nadu, India, *Agric. Econ.*, 25, 273–283, doi:10.1111/j.1574-0862.2001.tb00207.x.
- Serra, J. (1982), *Image Analysis and Mathematical Morphology*, 600 pp., Academic, London.
- Sharma, A. (2003), Rethinking tanks: Opportunities for revitalizing irrigation tanks—Empirical findings from Ananthapur district, Andhra Pradesh, India, *Working Pap.* 62, 16 pp., Intl. Water Manage. Inst., Colombo.
- Tauer, W., and G. Humborg (1993), *Irrigation par Ruissellement au Sahel: Télé-détection et Systèmes d'Information Géographique pour Déterminer des Sites Potentiels*, 192 pp., Cent. Tech. de Coop. Agricole et Rurale, Wageningen, Netherlands.
- Thiruvengadachari, S., and R. Sakthivadivel (1997), Satellite remote sensing for assessment of irrigation system performance: A case study in India, *Res. Rep.* 9, 23 pp., Int. Irrig. Manage. Inst., Colombo.
- Tideman, E. M. (1996), *Watershed Management: Guidelines for Indian Conditions*, 372 pp., Omega Sci., New Delhi.
- Vaidyanathan, A. (2001), *Tanks of South India*, 178 pp., Cent. for Sci. and Environ., New Delhi.

Y. Gunnell, Department of Geography, UMR 8591, CNRS, Université Paris VII-Diderot, Case Courrier 7001, 2 Place Jussieu, F-75205 Paris Cedex 13, France. (gunnell@paris7.jussieu.fr)

C. Mering and F. Mialhe, Department of Geography, UMR 8586, CNRS, Université Paris VII-Diderot, Case Courrier 7001, 2 Place Jussieu, F-75205 Paris Cedex 13, France.